Hierarchical collective motion of a mixture of active dipolar Janus particles and passive charged colloids in two dimensions

J. Harder and A. Cacciuto

Phys. Rev. E **97**, 022603 — Published 7 February 2018

DOI: 10.1103/PhysRevE.97.022603

Hierarchical Collective Motion of a Mixture of Active Dipolar Janus Particles and Passive Charged Colloids in Two Dimensions.

J. Harder and A. Cacciuto*

Chemistry Department,

Columbia University.

(Dated: January 10, 2018)

Abstract

We use computer simulations to study the behavior of a mixture of large passive charged colloids in a suspension of smaller active dipolar janus particles. We find that when a single charged colloid is present in solution, it acquires a rotational or translational motion depending on how the active dipoles self-assemble on its surface to form active complexes. The collective behavior of these complexes is quite remarkable, and includes swarming behavior and coherent macroscopic motion. We detail how the variety of different phenomenologies emerging in this system can ultimately be controlled by the strength of the active forces and the relative concentration of the two species.

* ac2822@columbia.edu

I. INTRODUCTION

Self-propelled particles convert energy from their surroundings into translational motion. This constant energy uptake results in a dynamics where each active particle, while still undergoing Brownian translational and rotational motion, can also move in the same direction with a persistence length of many times its own diameter [1–3]. Isotropic, hard self-propelled particles have been shown to have a remarkable collective behavior, ranging from the development of giant number fluctuations to motility induced phase separation [4–8]. Furthermore, they present an unusual behavior near surfaces and passive obstacles [9–16]. A key feature of systems of isotropic active particles is that there is no energy cost associated with the rotation of the particles within the self-assembled structures they form. While this rotational freedom is a crucial aspect of these particles' unusual behavior, the isotropy of the interactions greatly limits the structural properties of the aggregates they can form. The idea of using anisotropic particles whose orientations are coupled to those of their neighbors is as old as the field of active matter itself [17, 18], but it is only recently that long ranged aligning interactions have been considered in synthetic and colloidal systems, adding a phenomenological complexity to active particles ranging from turbulence to self-regulation and swarming behavior previously observed only in living systems (for recent reviews we refer the reader to [19–21] and the references therein).

Much of the numerical work in the field of active spherical colloids has focused on particles with isotropic potentials [22], and less has been done to explore how anisotropy in inter-particle interactions can affect the large scale collective dynamics of active systems. Spherical Dipolar Janus Particles (DJP) are the simplest colloidal entity with controllable surface interaction asymmetry. DJPs are composed of two hemispheres each functionalized with charged molecules of opposite sign, and they can be made to be passive [23], or active [24–29]. Passive DJPs present a rich phase behavior which includes the formation of dipolar clusters, linear assemblies and ring-like aggregates depending on the range and strength of the inter-particle interactions and concentration [30–37]. Recently, numerical simulations and experiments [19, 38–40] have indicated that a new level of dynamic and reconfigurable self-assembly complexity can be achieved when self-propelling DJPs under the influence of external fields. Inspired by these results, and by recent work on the behavior of passive components in active fluids [12, 41–44], we report numerical simulations of the complex

behavior of a mixture of Active Dipolar Janus Particles (ADJPs) and Passive Charged Colloidal (PCC) tracer particles. We show how the interplay between the strength of the active forces and that of the dipolar interactions can lead to a remarkable multi-stage dynamic self-assembly of the PCCs.

We begin this paper by introducing the models and the numerical methods used to gather our data. We then study the behavior of a suspension of pure ADJPs at different concentrations and activities. We next turn our attention to how a suspension of ADJPs interact with a single PCC. Finally, we consider the collective behavior of a mixture of multiple PCCs and ADJPs.

II. METHODS

Our simulations consist of a mixture of ADJPs, represented by disks of diameter σ with embedded point charges at area fractions ϕ_b, and PCCs represented as disks of diameter $\sigma_c = 10\sigma$ with a point charge at the particle center and area fraction ϕ_c. Both types of particles undergo over-damped Langevin dynamics, with the active dipoles having an additional term driving their self-propulsion with a force of strength F_a according to the equations:

$$m\ddot{\boldsymbol{r}} = -\gamma\dot{\boldsymbol{r}} - \nabla_{\boldsymbol{r}} V(r) + \sqrt{2\gamma^2 D}\xi(t) + F_a \boldsymbol{n} \tag{1}$$

$$\dot{\theta} = \sqrt{2D_r}\xi_r(t) \tag{2}$$

Here $\boldsymbol{n} = [\sin(\theta), \cos(\theta)]$ represents the orientation vector along which the active force is directed, γ is the friction coefficient, $V(r)$ the total potential acting on a particle, and D and D_r are the translational and rotational diffusion constants, respectively (with $D_r = 3D/\sigma^2$). The solvent-induced Gaussian white noise terms are given by $\langle \xi_i(t) \rangle = 0$, $\langle \xi_i(t) \cdot \xi_j(t') \rangle = \delta_{ij}\delta(t - t')$ and by $\langle \xi_r(t) \rangle = 0$, $\langle \xi_r(t) \cdot \xi_r(t') \rangle = \delta(t - t')$, for the translational and rotational motion respectively. All simulations are carried out using the numerical package LAMMPS [45], and throughout this work we use the default dimensionless Lennard-Jones units as defined in LAMMPS, for which the fundamental quantities mass m_0, length σ_0, epsilon ϵ_0, and the Boltzmann constant k_B are set to 1, and all of the specified masses, distances, and energies are multiples of these fundamental values corresponding to $T = T_0 = \epsilon_0/k_B$, $m = m_0$, $\sigma = \sigma_0$, and $\tau_0 = \sqrt{\frac{m_0\sigma_0^2}{\epsilon_0}}$ in our simulations.

The interaction potential between particles is the sum of a Weeks-Chandler-Andersen potential V_{WCA}, responsible for enforcing excluded volume between the disks, and electrostatic terms which depend on the particle type. The first term is given as

$$V_{\mathrm{WCA}}(r_{ij}) = 4\epsilon \left[\left(\frac{\sigma_{ij}}{r_{ij}} \right)^{12} - \left(\frac{\sigma_{ij}}{r_{ij}} \right)^{6} + \frac{1}{4} \right], \tag{3}$$

where the indices refer to the particle type, $\sigma_{ij} = (\sigma_i + \sigma_j)/2$, $\varepsilon = 5\varepsilon_0$, and the potential extends out to $2^{\frac{1}{6}}\sigma_{ij}$. The typical interaction potential between the two charged hemispheres of DJPs can be quite complicated to describe accurately, in particular when interactions are strongly screened by the presence of a salt and a simple dipolar description becomes inadequate [36, 46]. In this paper, however, we are not interested in the regime where particles are expected to self-assemble into isotropic dipole clusters, but in an intermediate regime where the dipolar character of the particles, although screened to some extent, still dominates their assembly, favoring the formation of elongated linear structures. We model this interaction by anchoring two explicit effective charges of opposite sign inside of each dipole. These charges are placed along the vector $\boldsymbol{n}$, at a distance $\pm 0.25\sigma$ from the center of the DJP, and rigidly translate and rotate with it. Similar models were used in [19, 32]. A single charge is placed at the center of each of the large passive colloids. Any two charges in the system interact according to:

$$V(r_{ij}) = \frac{q_i^{\mathrm{eff}} q_j^{\mathrm{eff}}}{\varepsilon_d r_{ij}} e^{-\kappa r_{ij}} \tag{4}$$

where the indices refer to the particle type, and q_i^{eff} is the effective charge they carry. The effective charges have been selected to provide typical interactions strengths observed in colloidal systems when at contact. Given our setup, we used $q^{\mathrm{eff}} = 10^4$ for the charged colloids, and $|q^{\mathrm{eff}}| = 5$ for the dipoles. Finally ϵ_d, and κ are set to 1 and $\beta = \mathbf{1}/(\mathbf{k_B T})$.

With this setup the attraction between two ADJP when co-aligned and sitting at the minimum of their interaction potential, V_0, is of the order of $10k_{\mathrm{B}}T$, specifically $V_0 \simeq 11.79k_{\mathrm{B}}T$. Throughout the paper, we will represent our results either in terms of $\beta F\sigma$, or in terms of $F\sigma/V_0$ where appropriate. The first term can be thought of as a Peclet number and gives direct information about the self-propelling velocity of the particles with respect to the thermal motion. The second term emphasizes the competition between the active forces in the system and the electrostatic dispersion forces between the dipoles. All simulations

are run **in a square box with periodic boundary conditions** for a minimum of 10^7 iterations with a time step $\Delta t = 10^{-3}\tau_0$ (where τ_0 is the dimensionless time). **To ensure an over-damped dynamics of the linear motion, we selected** $\gamma = 100\tau_0^{-1}$. Simulation snapshots and movies are rendered using VMD [47].

III. RESULTS AND DISCUSSION

We divide our results into sections where we first analyze the behavior of a suspension of ADJPs by themselves, we then study how these organize over the surface of a single passive charged colloid, and how different arrangements lead to different types of activated colloidal motion. Finally, we study the collective behavior of a mixture of multiple PCCs and ADJPs.

Suspensions of ADJPs

We begin our analysis by exploring the behavior of a suspension of ADJPs in the absence of charged colloids. Fig. 1 shows typical system configurations for different values of the active force, F_a and at different ADJP area fractions, ϕ_b.

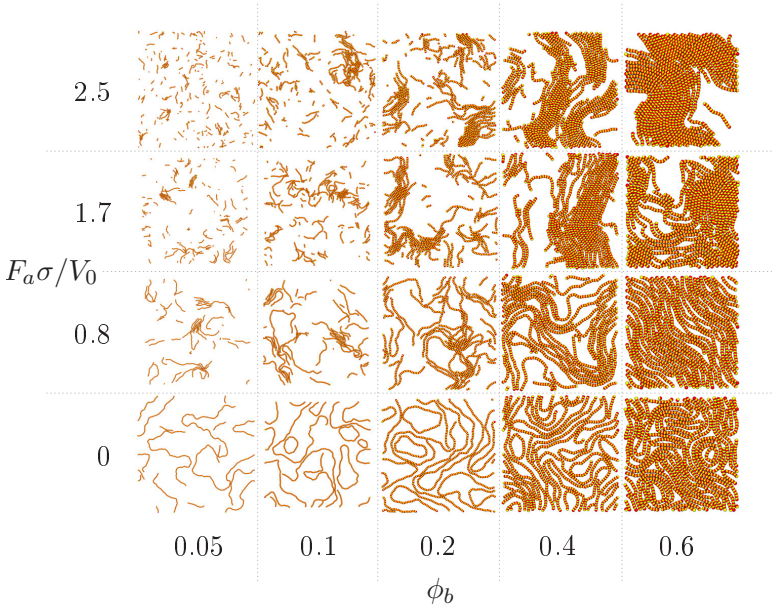

FIG. 1: Structural self-assembly diagram showing typical configurations acquired by active dipolar janus particles for a range of activities and particle area fractions. The self-propelling forces in this diagram have been rescaled by the ADJPs binding energy V_0.

Overall, we find that passive, weakly screened DJPs tend to self-assemble into closed loops or linear aggregates. Beyond a percolation threshold, the passive DJPs organize into a disordered network whose branches become thicker, but more tortuous as the area fraction of the DJPs increases. The introduction of a small amount of activity along the dipolar axis in a low density suspension leads to the formation of structures morphologically analogous to those of passive DJPs: loops and lines that now actively spin or slither across the system as a result of the coherent alignment of the active forces via electrostatic interactions. Overall, the length of these aggregates decreases as the swimming speed of their constituent particles increases. This is because flexible long chains are easily broken by the torques that develop from mis-aligned active forces within their backbone. In addition, swarming behavior similar to that seen in suspensions of active rods [48–50] is observed, albeit with smaller and smaller ADJP aggregates as F_a increases. The system is found in the fluid state of mostly isolated ADJPs as soon as $F_a\sigma/V_0$ becomes sufficiently large (not shown in the figure) to break apart all linear aggregates. Figure 2 shows how the average length of the ADJP chains decreases with the strength of the active forces in low area fraction suspensions. **These data are well described by an exponential decay of the form** $\langle n\rangle\sigma/L \sim \exp[-a(F_a\sigma/V_0)]$ **with** $a \simeq 2$**.**

For the largest area fractions considered here $\phi_b \geq 0.4$, a small amount of activity breaks the structure of the compressed network formed by the passive particles and generates ordered patterns of coherently moving linear aggregates that span the entire simulation box. Apart from the pattern for $\phi_c = 0.6$ and $F_a\sigma/V_0 = 0.8$ which seems to remain stable over the course of our simulations, the other patterns are transient as they form, break into smaller clusters, and then reform aperiodically over time. At these area fractions, larger activities tend to mostly compact the aggregates into fingerprint-like structures similar to those seen in active nematics [51].

Single Charged Colloid in a Suspension of ADJPs

Next, we consider the behavior of a low density bath of ADJPs in the presence of a single PCC. When a negatively charged large colloid is added to a bath of dipoles, DJP chains bind to the colloid forming radially extruding linear structures. In passive systems, we observe sparse coating of the colloid by a few long chains of dipoles, whereas ADJPs, moving in the

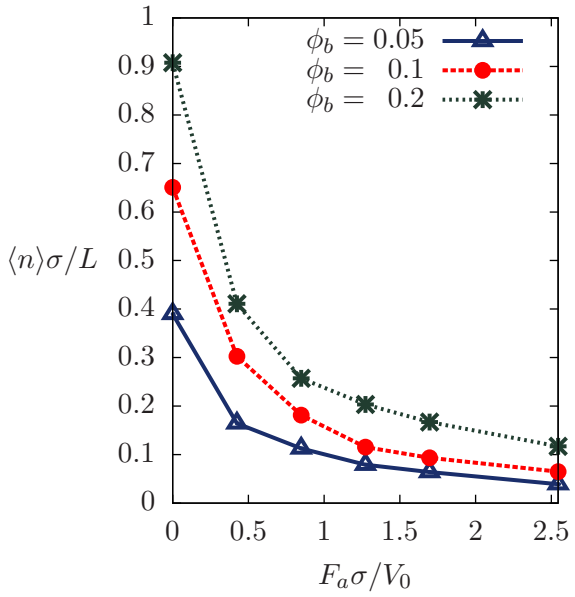

FIG. 2: The average ADJP chain length, normalized by the length of the simulation box L, as a function of the rescaled self-propelling force $F_a\sigma/V_0$, for different values of the particles' area fraction ϕ_b. $\langle n \rangle$ is the average size of clusters which are constructed by considering particles that are in contact with each other and for which their mutual orientation is off-set by an angle that is not larger than $\pi/6$.

direction of their minus-plus polar axis, cover the PCC surface more completely, albeit with shorter chains. Particle activity induces this change for two reasons: first, ADJP chains are shorter than passive ones so there are more chains in solution, and second, when the direction of the propelling axis is chosen so that the active force aligns with the direction of a favorable charge-dipole interaction (which is indeed the case in our simulations), the chains develop an effectively stronger binding attraction to the charged colloid than their bare electrostatic one, making the overall coverage of the colloidal surface by the chains more likely.

Two types of PCC-ADJP complexes form, depending on how much of the PCC surface is coated, with quite different behaviors. At low activity and high ϕ_b, adsorbed ADJP chains fully coat the PCC to form a polymer brush-like structure around it (see Fig. 3A), which we refer to as the 'corona'. Neighboring ADJP chains that densely coat the PCC have attractive lateral electrostatic interactions which make bundling favorable. The lowest energy configuration is one where all of the chains collapse around the PCC in the same direction and form a 'swirl' where the axis of ADJPs in the chains is tilted away from normal

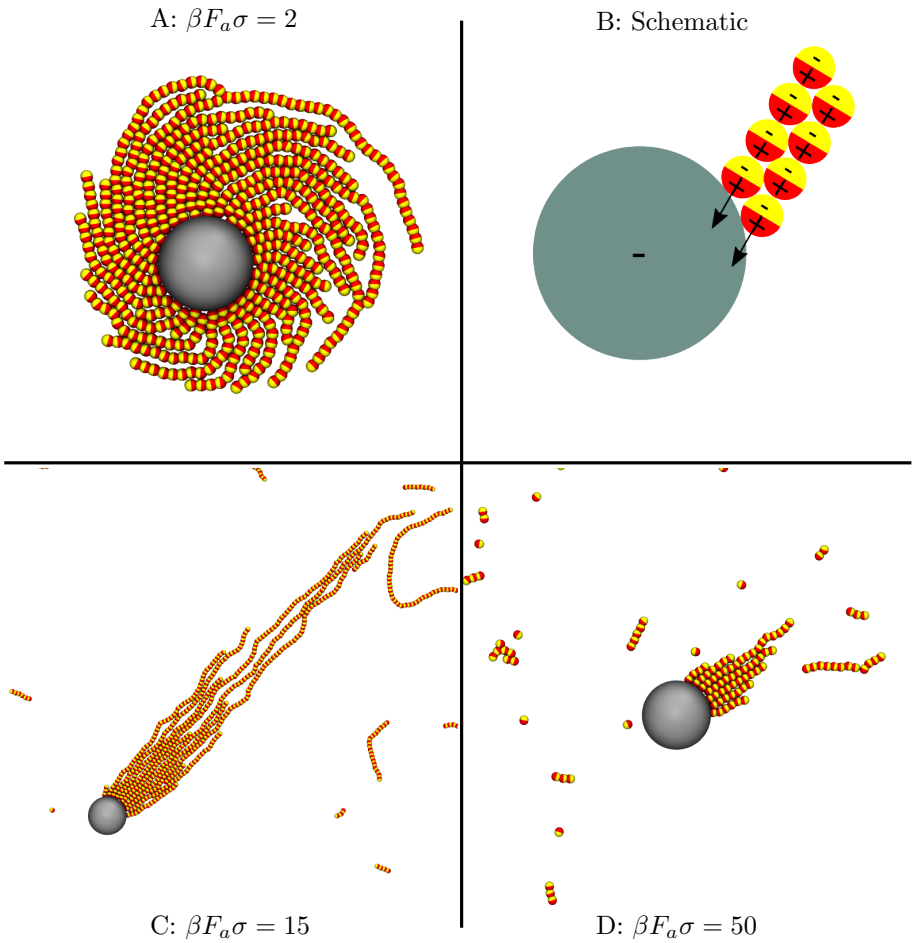

FIG. 3: A: Snapshot from simulations of a rotating brush of ADJPs chains over the surface of a PCC (see also supplementary movie S1 [52]). B: Idealized sketch showing how lateral interactions between ADJPs can lead to a tilt of the chain axis with respect to the surface of the PCC. This is responsible for the tangential active forces that lead to the rotation of the brush. C: Long tails of ADJPs developing over a PCC at low area fractions and intermediate activities. (supplementary movie S2 [52]) D: Short chains developing over a PCC at low area fractions and large activities.

to the PCC surface (Fig. 3B). When the DJPs are active, non-zero tangential components of the ADJP forces result in coherent rotations of the corona around the PCC. Thermal fluctuations and fluctuations in the chain lengths can occasionally change the handedness of the ADJP swirl, leading to a switching between clockwise and counterclockwise rotations. The persistence of these rotations in a specific handedness depends on the strength of the activity, the surface coverage, and the strength of the electrostatic interactions in a nontrivial

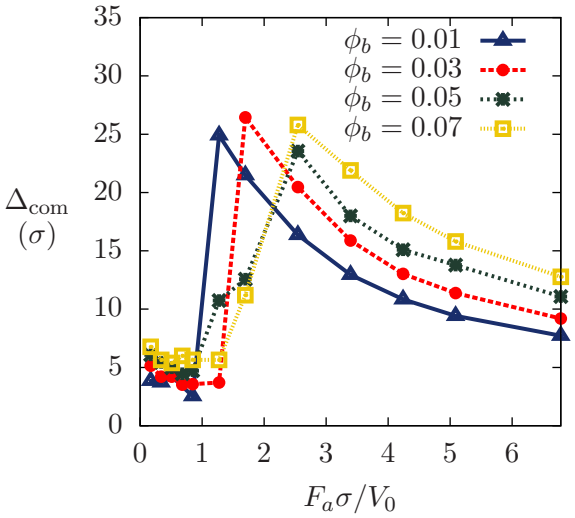

FIG. 4: Anisotropy of PCC-ADJP complexes, expresses in terms of $\Delta_{\rm com}$ (see text for a definition of $\Delta_{\rm com}$), as a function of the strength of the active forces, here represented in the rescaled form $F_a\sigma/V_0$, and for different values of the ADJP area fraction ϕ_b.

manner. The PCC is rarely coated by chains of identical length, so in addition to the rotation of the corona, the PCC is propelled as an activated particle with force having strength and direction that depends on the fluctuating balance of forces induced by the adsorbed active chains. In this configuration, the PCC-ADJP complex tends to move in tight circles of varying radius and handedness similar to the motion recently observed in [53].

A rather different PCC-ADJP complex forms in the limit of a sufficiently large self-propelling force and low ADJP concentration. In this regime, the PCC is no longer evenly or fully coated. Any asymmetric coverage results in a clear imbalance of forces that translationally propels the colloid in a specific direction. Once a bare patch on the PCC surface is formed, especially at low ϕ_b, it is rare that the colloid becomes fully coated again. The partially coated PCC now effectively becomes an active particle whose source of propulsion is a tail of ADJP chains which are kept in a bundle by lateral dipole interactions (see Fig. 3C and D). Over time, these trailing chains grow away from the direction of motion through the addition of free ADJP chains from solution, or by the incorporation of ADJPs that initially bind to the bare face of the now mobile PCC, and subsequently slide around the colloid to merge with the pre-existing pushing chains. The trailing chains can grow to lengths that can be significantly larger than the diameter of the colloid.

A single parameter allows us to both differentiate fully coated from partially coated

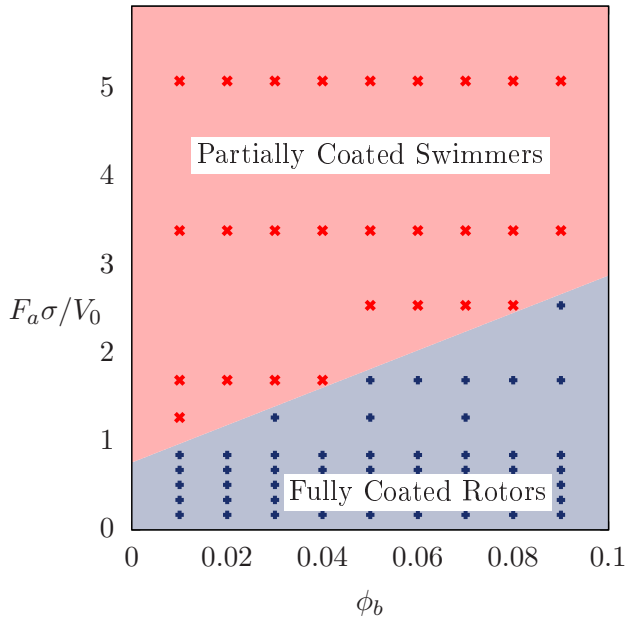

FIG. 5: Structural phase diagram showing where a charged colloid is fully and partially coated for different values of the rescaled active force $F_a\sigma/V_0$ and ADJP area fraction ϕ_b. As the area fraction increases at a given bath activity, the charged colloid is more readily fully coated. At the border between the two regions, the charged colloid can alternate between being fully and partially coated, especially at higher ADJP area fractions, ϕ_b. The line separating the two regimes is a guide to the eye.

PCCs as well as explore the properties of the ADJP chains that are bound to partially coated colloids. We define Δ_{com} as the distance between the center of the colloid and the center of mass of all of the dipoles which are connected directly (via contact), or indirectly (through the ADJP chains) to the PCC. Figure 4 shows how Δ_{com} depends on the strength of the active forces at different values of ϕ_b. **Interestingly for** $F_a\sigma/V_0 < 1$ the center of mass of the corona is close to the center of the PCC, indicating that the PCC is fully coated by chains of roughly equal length (Fig. 3A). **As the active forces become larger than the dispersion forces,** $F_a\sigma/V_0 \gtrsim 1$, a sudden jump in Δ_{com}, corresponding to the transition from a fully coated to a partially coated PCC (Fig. 3C), is observed. The location of this jump shifts to larger activities for higher ϕ_b, where ADJPs can fully coat the colloid more easily. As the activity increases further, the asymmetry decreases from its maximum value because, as in the system consisting of only ADJPs, chains break up more easily giving rise to shorter adsorbed tails (Fig. 3D).

We summarize these results with the structural phase diagram in Fig. 5 showing how for our specific set of electrostatic interactions, the extent to which the PCC is coated depends on the strength of the active forces and the area fraction of the ADJPs in solution. Above $\phi_b \approx 0.05$, and for propelling forces near the structural phase diagram boundary, the system shows bistable behavior where a PCC alternates repeatedly between being a fully coated colloid with a rotating corona, and a partially coated translational swimmer, somewhat reminiscent of the motion of run-and-tumble bacteria.

Starting simulations at small values of ϕ_b, low values of $F_a\sigma/V_0$ and with all particles randomly distributed, the PCC is initially partially coated and can remain so for long times. Once the PCC becomes fully coated, however, the ADJP swirl structure is very stable. Conversely when simulations are initialized in a configuration where the PCC is fully and densely coated, the rotating corona phase persists to higher ADJP activities at a given ϕ_b, but once the activity is sufficiently large the corona breaks up and the colloid becomes partially coated.

Rotational Dynamics of a Swirl of ADJPs

In this section, we consider the rotational dynamics of the fully coating corona of ADJPs over the colloid. In Fig. 6 we track the typical dependence of the global angular displacement of the ADJP swirl $(\theta(t) - \theta(0))$ over time for different values of the active force. At low activities, the sign of the rotational velocity of the swirl does not change often, indicating that the ADJP rotations persist with the same handedness for long times. As the activity increases, this persistence time decreases while the rotational speed of the corona increases. There is no bias in favor of rotation in any particular direction, so at very long times, the total rotation of the corona is diffusive. The inset in Fig. 6 shows the average persistence time of this rotational motion in a specific handedness $\langle t \rangle$ as a function of F_a. These data are well characterized by a simple exponential function of the type $e^{-\alpha\beta F_a\sigma}$ with $\alpha \approx 0.5$. The corona changes direction through collisions with unbound chains in solution as well as through internal structural rearrangements. At low activities, electrostatic chain-chain interactions dominate and adsorbed ADJPs chains are the longest, thus leading to the largest values of $\langle t \rangle$. For larger values of F_a, the ADJP chains are shorter and can rearrange more easily. As a result, the active motion of the ADJPs becomes more important relative to

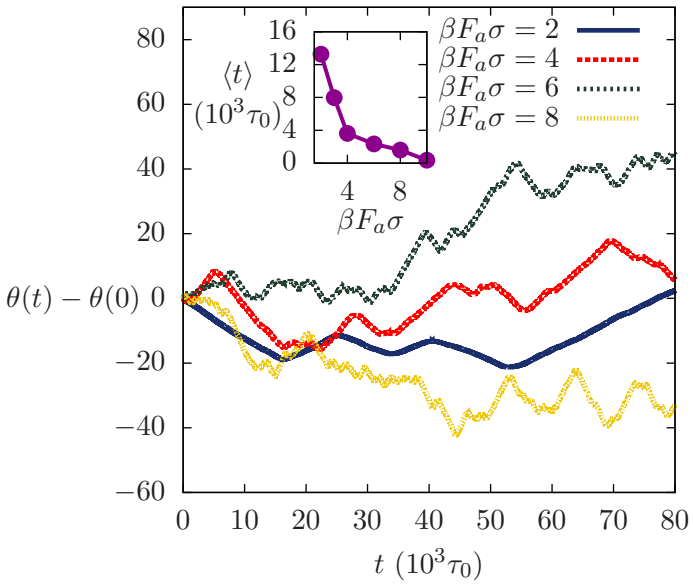

FIG. 6: Total angular displacement of the ADJP brush (corona) around a charged colloid as a function of time for $\phi_b = 0.03$. The inset shows the average time $\langle t \rangle$ spent by the corona rotating with a given handedness as a function of the self-propelling force F_a. As a reference, for all these activities $F_a\sigma/V_0 < 1$, and at this value of ϕ_b the system is stable in the fully coated rotor state as shown in Fig. 5.

their electrostatic interactions, leading to overall smaller values of $\langle t \rangle$. With increasing ϕ_b at a given F_a, ADJP chains grow longer and $\langle t \rangle$ generally increases.

Induced Active Motion of a PCC

In this section, we explore the dynamics of a single partially coated activated PCC. Typical two-dimensional trajectories of the PCC at low ϕ_b, and for values of F_a where the colloid is partially coated, plotted over the same amount of time (Fig. 7) show that the motion of the PCC-ADJP complex is strongly linked to the properties of the ADJP bath. In a bath with low activity, the motion of the aggregate persists in the same direction for very long times. As F_a increases, the net distance traveled by the aggregate increases, but the persistence length of its trajectory becomes smaller.

The orientational correlation function of the PCC swimming direction, $R_{\boldsymbol{uu}} = \langle \boldsymbol{u}(0)\boldsymbol{u}(t)\rangle / \langle \boldsymbol{u}(0)^2 \rangle$, where $\boldsymbol{u}(t)$ is the normalized displacement vector of the PCC between any two successive time steps of size $100\tau_0$, reflects the roughening of the PCC-

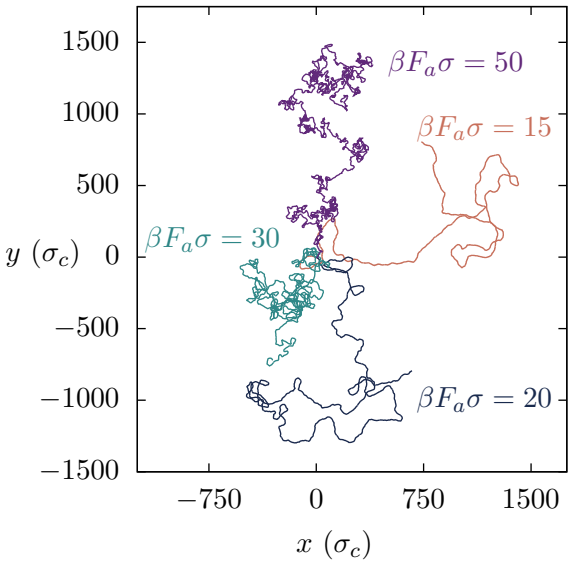

FIG. 7: Typical trajectories of a PCC partially coated by a bundle of ADJPs for four different values of F_a over the same elapsed time. As the bath particle activity increases, the trajectories become rougher. This trajectories were takes at a ADJP area fraction $\phi_b = 0.01$.

ADJP trajectory with increasing F_a (Fig. 8A), and helps to explain some of the dynamics of the activated tracer. The rotational dynamics of the PCC-ADJP complex is mostly diffusive when the dipoles do not organize into a corona, but rather into a linear bundle, therefore a simple exponential fit to the orientational correlation functions allows us to directly extract the effective rotational diffusion coefficient, D_r^{eff}, of the complex at different ADJP activities (shown Fig. 8B). The reason for the increase of D_r^{eff} with F_a is not immediately obvious because, in principle, the rotational diffusion of an isolated active particle depends only on the temperature and not on the strength of the active forces. In this case, however, the activated PCC is not an isolated particle, but is propelled by a tail of ADJPs of length, $\ell \propto \Delta_{\text{com}}$, which is inversely dependent on F_a (see Fig. 4). In this case, it is useful to think of the PCC-ADJP complex as a rod-like object for which the rotational diffusion coefficient D_r^{eff} is expected to scale as ℓ^{-3}. This is consistent with our results, shown in Fig. 8C, where we plot D_r^{eff} as a function of Δ_{com}. A power-law fit to the data with ax^{-b} at a value of $\phi_b = 0.01$ leads to an exponent $b = 3.1 \pm 0.2$, indicating that indeed, a PCC-ADJP complex with a long tail of ADJPs (low F_a) rotates more slowly than one with a short tail (high F_a). Interestingly, at higher values of ϕ_b the value of the fit exponent remains fairly

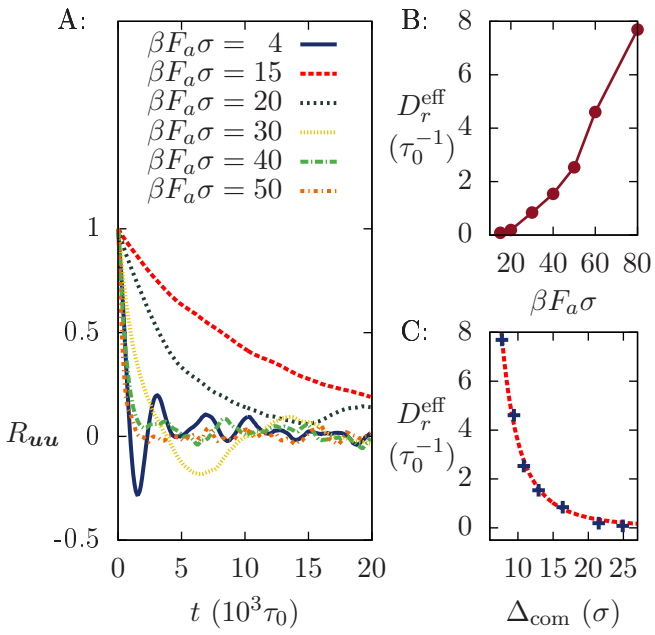

FIG. 8: A: Orientational correlation functions for the normalized displacement vector $\boldsymbol{u}(t)$ of a partially coated PCC-ADJP complex at $\phi_b = 0.01$. B: Effective rotational diffusion coefficients of a PCC-ADJP complex measured by fitting an exponential to the orientational correlation functions presented in A. C: Rotational diffusion coefficients of the PCC-ADJP complex as a function of the chain length $\propto \Delta_{\rm com}$. The dotted line is a power-law fit to the data.

compatible with our model of the aggregate as a rotationally diffusing rod ($b = 2.6 \pm 0.2$ for $\phi_b = 0.05$), though at these values of ϕ_b, more collisions between the aggregate and unbound ADJP chains occur, complicating the rotational dynamics of aggregate. Larger deviations are expected at even larger area fractions.

For completeness, we include the orientational correlation function of a fully coated PCC ($\beta F_a\sigma = 4$) in Fig. 8A. The periodic behavior of the orientational correlation function suggests that the rotational motion of the ADJP swirl forces the colloid to move in rough circles, as we indeed observe in our simulations. The net active force on these fully coated colloids is much lower than that on a partially coated particle, so they move at a significantly lower speed. Nevertheless, even the motion of the fully coated PCC can be considered as activated when compared to that of a colloid in a passive bath.

In summary, a bath of active dipoles can effectively turn a passive charged colloid into an active colloid whose motion depends strongly on the assembly properties of the ADJPs

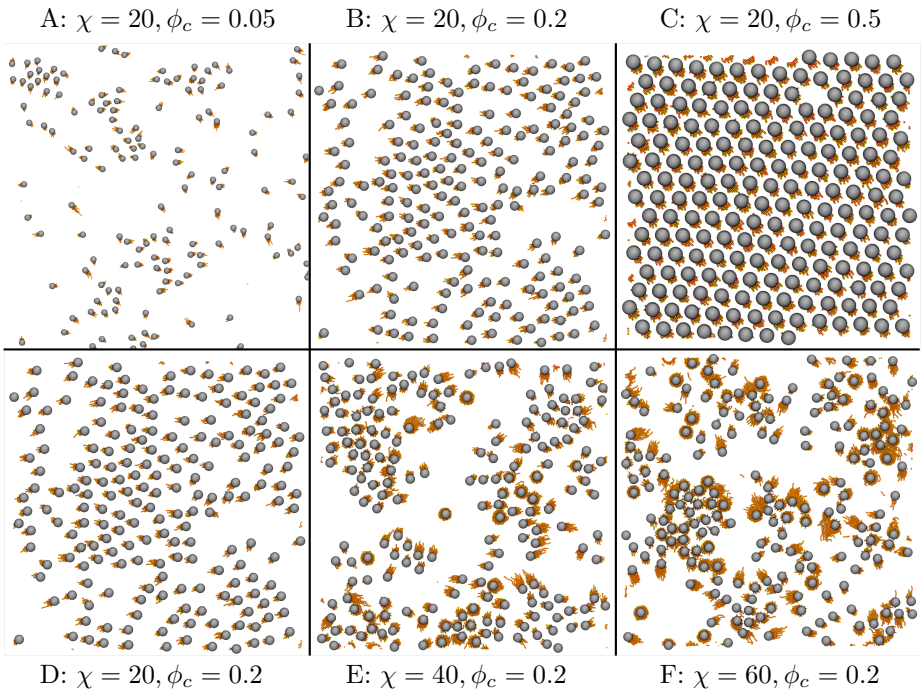

FIG. 9: Top: Snapshots of steady state configurations taken from simulations for different values of PCC area fraction ϕ_c at a fixed value of $F_a\sigma/V_0 = 1.7$ and number of ADJP per PCC, $\chi = 20$. ϕ_c increases when going from A to C (supplementary movie S3 [52]). Bottom: Snapshots of steady state configurations taken from simulations for different values of χ at constant PCC area fraction $\phi_c = 0.2$ and a fixed value of $F_a\sigma/V_0 = 1.7$. χ increases when going from D to F.

on its surface. At low activities, the PCC moves aperiodically in circles as a swirl of active dipoles rotates around it. At intermediate bath activities, the PCC is pushed in the same direction for very long times by a bundle of long chains of ADJPs that only partially coat the PCC surface. As the activity is increased further, the size of the ADJP tail decreases, inter-particle interactions become less important compared to the self-propelled motion of the ADJPs, and the PCC begins to move more like a tracer particle in an active bath, diffusively but with an enhanced diffusion coefficient [54–56].

Multiple Colloids

In the previous sections we showed that by using ADJPs it is possible to turn a single isotropic, passive colloid into an anisotropic, active one. In this section we investigate the

collective behavior of these activated colloids. We perform simulations with $N_c = 200$ PCCs at different values of ϕ_c with different numbers of ADJPs per PCC, a quantity we define as χ, ranging from $\chi = 20$ to $\chi = 60$ (and several simulations with fewer colloids at higher values of χ). As a reference, with the electrostatic interaction parameters that we have chosen for this study, in the absence of ADJPs, a solution of PCCs forms a hexagonal structure above $\phi_c^* \approx 0.3$.

In these simulations, the values of χ and ϕ_c can be used to create or destroy both structural order and coherent motion in PCCs. Simulation snapshots in the top row of Fig. 9(A-C) show typical configurations at a fixed $F_a\sigma/V_0 = 1.7$ and $\chi = 20$ for increasing colloidal densities. At the lowest densities, dynamic groups of PCC-ADJP complexes show swarming behavior, where the orientation of the complexes (and thus their motion) is correlated only between nearby complexes. As ϕ_c increases, most of the complexes have the same orientation, where the center of mass of the particles translates in one direction with little order within a fluid of partially coated PCCs. At sufficiently high ϕ_c, the PCC-ADJP complexes form an ordered crystal with center of mass that moves according to the average orientation of the complexes. A key requirement for coherent PCC motion is that χ is small enough so that when the ADJPs are partitioned evenly among the PCCs, none of the colloids are fully coated, and crucially, few or none are uncoated. In other words all of the PCCs must be activated. If this is the case, then electrostatic interactions can reorient neighboring particles so that they move in the same direction. While increasing ϕ_c increases the order in the system, simply increasing the extent by which ADJPs can coat PCCs can reduce, and even destroy the coherent motion of the complexes. This is illustrated in the bottom row of Fig. 9(D-F), where we show snapshots of typical configurations with increasing number of ADJP per colloid, χ, at a fixed density $\phi_c = 0.2$ and $F_a\sigma/V_0 = 1.7$.

To quantitatively account for the coherency of the particle motion we measure the order parameter ψ defined as

$$\psi = \frac{1}{N_c}|\sum_{i=0}^{N_c} \boldsymbol{\mu}_i| \tag{5}$$

where $\boldsymbol{\mu}_i$ is the unit vector along the axis connecting the center of mass of the colloid to the center of mass of the dipoles bound to that colloid (the direction associated with Δ_{com}), and the sum runs over all PCC-ADJPs complexes in the system [18]. In Fig. 10, we plot the orientational order parameter of the PCC-ADJP complexes as a function of χ for different

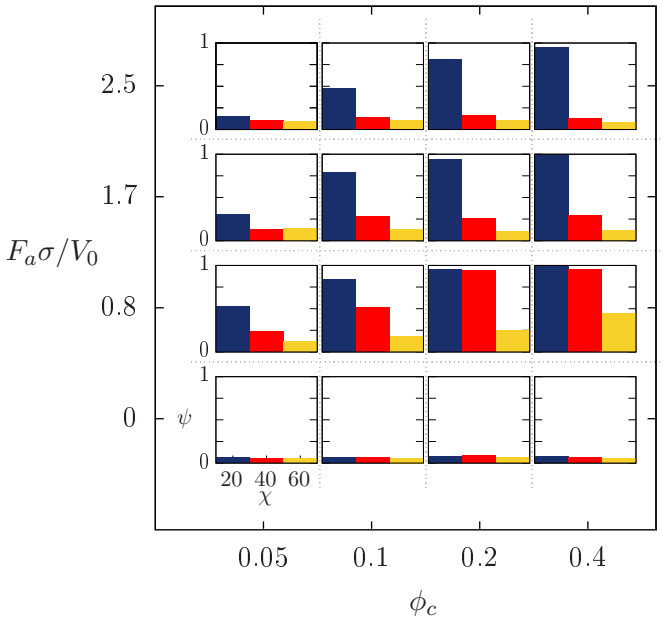

FIG. 10: Matrix of figures showing the order parameter ψ associated with the motion of the PCC-ADJP complexes for three different values of the number of ADJP per PCC, χ; $\chi = 20$, $\chi = 40$ and $\chi = 60$. Each panel shows the same data for different values of PCC area fractions ϕ_c and rescaled active forces $F_a\sigma/V_0$

values of $F_a\sigma/V_0$ and ϕ_c. At low ϕ_c the motion of PCC-ADJP complexes is relatively uncorrelated regardless of the value of χ, albeit with a larger degree of order for small χs − a trend that persists throughout the phase diagram. As ϕ_c increases for $F_a\sigma/V_0 < 1$, the small χ complexes develop a coherent, macroscopic ordered motion ($\chi = 20$, shown in blue). For identical conditions, systems with larger surface coverage have significantly less coherent motion, an effect that becomes even more pronounced as the average PCC surface coverage increases beyond $\chi = 60$ (not shown). Overall, as the activity increases and $F_a\sigma/V_0$ becomes significantly larger than 1, the orientational order in the system decreases. We also confirm this for the case of $\chi = 20$ in a system with $\phi_c = 0.4$ and $F_a\sigma/V_0 = 4.25$, where we measure $\psi = 0.27$ (not shown in the figure). For intermediate values of χ, there is a regime, at low activity and high ϕ_c, where the colloids are pushed in the same direction and can swim in an orderly manner. However, as soon as the colloids can become fully coated, as is the case in systems with $\chi = 60$, PCC-ADJPs complexes do not show any significant coherent motion, as fully coated colloids are relatively passive. At these values of χ the system separates into fully coated and partially coated PCC-ADJPs complexes.

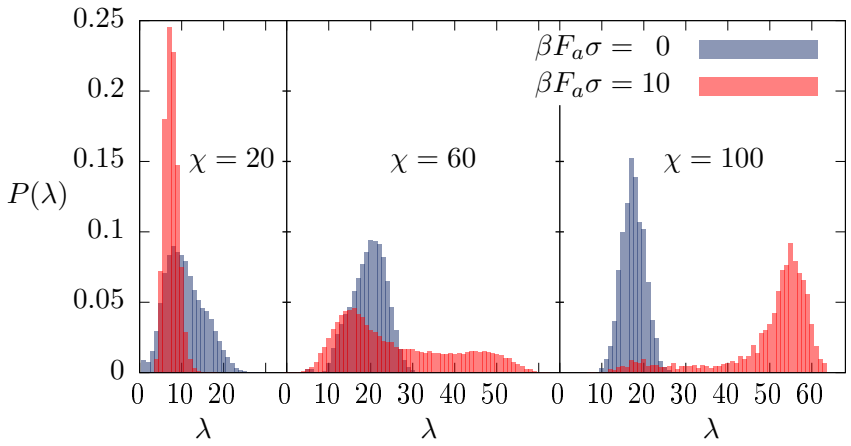

FIG. 11: Distribution of the number of ADJP chains bound to the surface of the PCCs, $P(\lambda)$, for a passive and an active ($\beta F_a\sigma = 10$) suspension at different values of number of ADJPs per PCC, χ.

The coherence of the PCC motion is related to the distribution of ADJPs bound to the surface of each PCC, $P(\lambda)$, which has a nontrivial dependence on the value of χ. In this respect, it is instructive to look at the distribution of adsorbed ADJPs over the surface of the PCCs. Remarkably, at moderate activities, large ϕ_c and small $\chi = 20$, i.e. when the colloids acquire a collective coherent motion, the width of the distribution of ADJPs across the PCCs is much narrower than it is in the parent passive system (Fig. 11, left). We believe that this is due to a self-regulation effect where, the PCC-ADJPs complexes exchange ADJPs so that all of the colloids are activated and move at roughly the same speed, so that particles can maintain a constant distance from each other, thus decreasing their mutual electrostatic repulsive energy. Upon increasing the number of ADJPs per colloid in solution to $\chi = 60$, we find that the distribution becomes bimodal (see Fig. 11, middle). In this case we observe a mixture of fully coated and partially coated PCCs. A further increase of χ eventually leads to the full coating of all of the PCCs. This trend is already visible for $\chi = 100$ (in Fig. 11, right) where most of the particles develop a full isotropic coating of ADJPs. This behavior is consistent with what observed in Fig. 5. As one moves at a constant propelling force and ϕ_c from small to large values of χ, one goes from partially coated, through mixed, to fully coated PCC-ADJPs complex configurations. Interestingly, the repulsive interactions between the fully coated PCCs are somewhat screened by the ADJP chains, and so the resulting PCC-ADJP complexes are less repulsive than the bare PCCs. This interaction is

mediated by the chains of ADJPs coming from different particles that can align with each other forming transient attractive bonds between the particles. See supplementary material (S4 [52]) for an example showing the dynamics for this case.

IV. CONCLUSIONS

In this paper we have presented extensive simulations of a system of large, passive and charged colloids in a bath of small active dipolar janus particles. We believe this is one of the first examples of activity driven multi-stage self-assembly, where the strength of the propelling forces not only controls how ADJPs self-assemble over the surface of passive colloids, but also determines and regulates the collective behavior of PCC-ADJP complexes via self-regulatory ADJPs exchange. The PCC-ADJP complexes that spontaneously develop in these systems as a result of the electrostatic interactions between the different components acquire a net directional motion whenever the colloidal surface is not fully coated by the ADJPs, and a spiraling motion when it is fully coated. In the first case, the ADJPs form long chains that bundle on one side of the charged colloid. In the second case, we observe the formation of a fully coating brush of ADJPs chains, which rotates coherently over the colloidal surface. **At low volume fractions, the onset between the two phases occurs when** $F_a\sigma/V_0 \simeq 1$. In both cases, the persistence length of the activated colloidal trajectories is controlled by the strength of the active forces.

We believe that the coherent rotation of the corona of dipoles over the surface of the particles observed in our system is, to a certain extent, similar to the phenomenology reported by Czirók et. al. [57]. Here, a system of Vicsek particles constrained to move over a straight line with periodic boundary conditions was found to develop a kinetic phase transition characterized by global particle alignment. In our study, we do see global alignment of the linear aggregates of dipoles as well, but in all cases the handedness of the rotational motion eventually switches around. We believe that this is because of the finite-sized nature of our system, characterized by a relative small number of dipoles per colloid, but also because of the significant fluctuations in chain lengths, and because the dipole-dipole interactions between the chains tend to favor specific tilt angles rather than arbitrary ones.

We have also studied the collective behavior of PCC-ADJP complexes that develop upon immersing a number of PCCs in a bath of ADJPs. Remarkably, we observe that at sufficiently large PCC densities and for a range of ADJP concentrations, a coherent swimming behavior of the complexes ensues due to a partitioning of ADJPs among the PCCs which narrows the natural (equilibrium) distribution of DJP chains per colloid. Interestingly, preliminary results also suggest that moderately dense systems of PCCs with a large number of ADJPs can develop attractive interactions due to chains interactions and interdigitation.

Overall, we expect the size and charge of the PCCs to be important parameters that control the structural phase behavior of the complexes, and in this respect, it is worth noting that we observed the formation of a rotating corona also in simulations performed with a PCC half the size of the ones discussed in this paper ($\sigma_c = 5\sigma$), and with an embedded point charge chosen to obtain comparable charge-dipole interactions at the colloidal surface.

As is the case for all active systems, we expect hydrodynamics to play a non-trivial role, possibly leading to enhanced coupling of the motion of particle complexes and of the self-assembled ADJP chains. Furthermore, our simple model neglects possible effects due to charge polarization and many-body interactions mediated by the presence of salt and counter-ions that could to some degree affect the self-assembled structures. More work to understand the role of these electrostatic effects in an active environment with explicit hydrodynamic interactions is needed, and will be the subject of a future study.

V. ACKNOWLEDGMENTS

We thank Stewart Mallory and Clarion Tung for insightful discussions and helpful comments. A.C. acknowledges financial supported from the National Science Foundation under Grant No. DMR-1408259.

---

[1] S. J. Ebbens, Current Opinion in Colloid & Interface Science **21**, 14 (2016).

[2] K. K. Dey and A. Sen, Journal of the American Chemical Society (2017), 10.1021/jacs.7b02347.

[3] W. Wang, W. Duan, S. Ahmed, T. E. Mallouk, and A. Sen, Nano Today **8**, 531 (2013).

[4] M. E. Cates and J. Tailleur, Annual Review of Condensed Matter Physics **6**, 219 (2015).

[5] S. Takatori, W. Yan, and J. Brady, Physical Review Letters **113**, 028103 (2014).

[6] C. Bechinger, R. Di Leonardo, H. Lwen, C. Reichhardt, G. Volpe, and G. Volpe, Reviews of Modern Physics **88**, 045006 (2016).

[7] J. Palacci, S. Sacanna, A. P. Steinberg, D. J. Pine, and P. M. Chaikin, Science **339**, 936 (2013).

[8] Y. Fily and M. C. Marchetti, Physical Review Letters **108**, 235702 (2012).

[9] S. A. Mallory, A. ari, C. Valeriani, and A. Cacciuto, Physical Review E **89** (2014), 10.1103/PhysRevE.89.052303.

[10] Y. Fily, A. Baskaran, and M. F. Hagan, Phys. Rev. E **91**, 012125 (2015).

[11] L. Baraban, D. Makarov, R. Streubel, I. Mnch, D. Grimm, S. Sanchez, and O. G. Schmidt, ACS Nano **6**, 3383 (2012).

[12] N. Koumakis, A. Lepore, C. Maggi, and R. D. Leonardo, Nature Communications **4**, ncomms3588 (2013).

[13] R. Ni, M. A. Cohen Stuart, and P. G. Bolhuis, Physical Review Letters **114**, 018302 (2015).

[14] R. Di Leonardo, L. Angelani, D. DellArciprete, G. Ruocco, V. Iebba, S. Schippa, M. P. Conte, F. Mecarini, F. De Angelis, and E. Di Fabrizio, Proc. Natl. Acad. Sci. USA **107**, 9541 (2010).

[15] C. Maggi, J. Simmchen, F. Saglimbeni, J. Katuri, M. Dipalo, F. De Angelis, S. Sanchez, and R. Di Leonardo, Small **12**, 446 (2016).

[16] A. Pototsky, A. M. Hahn, and H. Stark, Phys. Rev. E **87**, 042124 (2013).

[17] C. W. Reynolds, in *Proceedings of the 14th Annual Conference on Computer Graphics and Interactive Techniques*, SIGGRAPH '87 (ACM, New York, NY, USA, 1987) pp. 25–34.

[18] T. Vicsek, A. Czirk, E. Ben-Jacob, I. Cohen, and O. Shochet, Physical Review Letters **75**, 1226 (1995).

[19] S. H. L. Klapp, Current Opinion in Colloid & Interface Science **21**, 76 (2016).

[20] M. C. Marchetti, Y. Fily, S. Henkes, A. Patch, and D. Yllanes, Current Opinion in Colloid & Interface Science **21**, 34 (2016).

[21] M. C. Marchetti, J. F. Joanny, S. Ramaswamy, T. B. Liverpool, J. Prost, M. Rao, and R. A. Simha, Reviews of Modern Physics **85**, 1143 (2013).

[22] P. Romanczuk, M. Br, W. Ebeling, B. Lindner, and L. Schimansky-Geier, The European Physical Journal Special Topics **202**, 1 (2012).

[23] A. Walther and A. H. E. Mller, Chemical Reviews **113**, 5194 (2013).

[24] I. Buttinoni, G. Volpe, F. Kmmel, G. Volpe, and C. Bechinger, Journal of Physics: Condensed Matter **24**, 284129 (2012).

[25] H.-R. Jiang, N. Yoshinaga, and M. Sano, Physical Review Letters **105**, 268302 (2010).

[26] S. Jiang, Q. Chen, M. Tripathy, E. Luijten, K. S. Schweizer, and S. Granick, Advanced Materials **22**, 1060 (2010).

[27] J. Zhang, B. A. Grzybowski, and S. Granick, Langmuir **33**, 6964 (2017).

[28] W. Gao, A. Pei, X. Feng, C. Hennessy, and J. Wang, Journal of the American Chemical Society **135**, 998 (2013).

[29] J. N. Johnson, A. Nourhani, R. Peralta, C. McDonald, B. Thiesing, C. J. Mann, P. E. Lammert, and J. G. Gibbs, Physical Review E **95**, 042609 (2017).

[30] D. M. Rutkowski, O. D. Velev, S. H. L. Klapp, and C. K. Hall, Soft Matter **13**, 3134 (2017).

[31] B. Bharti and O. D. Velev, Langmuir **31**, 7897 (2015).

[32] H. Schmidle, C. K. Hall, O. D. Velev, and S. H. L. Klapp, Soft Matter **8**, 1521 (2012).

[33] B. Ren, A. Ruditskiy, J. H. K. Song, and I. Kretzschmar, Langmuir **28**, 1149 (2012).

[34] S. K. Smoukov, S. Gangwal, M. Marquez, and O. D. Velev, Soft Matter **5**, 1285 (2009).

[35] Q. Chen, J. K. Whitmer, S. Jiang, S. C. Bae, E. Luijten, and S. Granick, Science **331**, 199 (2011).

[36] L. Hong, A. Cacciuto, E. Luijten, and S. Granick, Nano Letters **6**, 2510 (2006).

[37] L. Hong, A. Cacciuto, E. Luijten, and S. Granick, Langmuir **24**, 621 (2008).

[38] A. Kaiser, K. Popowa, and H. Lwen, Physical Review E **92**, 012301 (2015).

[39] J. Yan, M. Han, J. Zhang, C. Xu, E. Luijten, and S. Granick, Nature Materials **15**, 1095 (2016).

[40] F. Guzmn-Lastra, A. Kaiser, and H. Lwen, Nature Communications **7** (2016), 10.1038/ncomms13519.

[41] S. A. Mallory, C. Valeriani, and A. Cacciuto, Physical Review E **90**, 032309 (2014).

[42] J. Simmchen, A. Baeza, D. Ruiz, M. J. Esplandiu, and M. Vallet-Reg, Small **8**, 2053 (2012).

[43] S. Sundararajan, P. E. Lammert, A. W. Zudans, V. H. Crespi, and A. Sen, Nano Letters **8**, 1271 (2008).

[44] E. W. Burkholder and J. F. Brady, Physical Review E **95**, 052605 (2017).

[45] S. Plimpton, Journal of Computational Physics **117**, 1 (1995).

[46] M. C. Hagy and R. Hernandez, The Journal of Chemical Physics **137**, 044505 (2012).

[47] W. Humphrey, A. Dalke, and K. Schulten, Journal of Molecular Graphics **14**, 33 (1996).

[48] M. Abkenar, K. Marx, T. Auth, and G. Gompper, Physical Review E **88**, 062314 (2013).

[49] Y. Yang, V. Marceau, and G. Gompper, Physical Review E **82**, 031904 (2010).

[50] H. H. Wensink and H. Lwen, Journal of Physics: Condensed Matter **24**, 464130 (2012).

[51] S. J. DeCamp, G. S. Redner, A. Baskaran, M. F. Hagan, and Z. Dogic, Nature Materials **14**, 1110 (2015).

[52] See Supplemental Material at URL for movies taken from sample simulations..

[53] C. A. Velasco, S. D. Ghahnaviyeh, H. N. Pishkenari, T. Auth, and G. Gompper, Soft Matter (2017), 10.1039/C7SM00439G.

[54] A. Morozov and D. Marenduzzo, Soft Matter **10**, 2748 (2014).

[55] X.-L. Wu and A. Libchaber, Physical Review Letters **84**, 3017 (2000).

[56] C. Valeriani, M. Li, J. Novosel, J. Arlt, and D. Marenduzzo, Soft Matter **7**, 5228 (2011).

[57] A. Czir´k, A.-L. Barabàsi, and T. Vicsek, Physical Review Letters **82**, 209 (1999).